Hydrology Research

Hydrology Research Vol 53 No 9, 1129 doi: 10.2166/nh.2022.201

Multilayer blue-green roofs as nature-based solutions for water and thermal insulation management

Elena Cristiano [a,*], Antonio Annis [b], Ciro Apollonio [c], Dario Pumo [d], Salvatore Urru [a], Francesco Viola [a], Roberto Deidda [a], Raffaele Pelorosso [c], Andrea Petroselli [e], Flavia Tauro [f], Salvatore Grimaldi [f], Antonio Francipane [d], Francesco Alongi [d], Leonardo Valerio Noto [d], Olivier Hoes [g], Friso Klapwijk [h], Brian Schmitt [h] and Fernando Nardi [b,i]

[a] Dipartimento di Ingegneria Civile, Ambientale e Architettura, Università degli Studi di Cagliari, Cagliari, Italy
[b] WARREDOC, Università per Stranieri di Perugia, Perugia, Italy
[c] Dipartimento DAFNE, Università degli Studi della Tuscia, Viterbo, Italy
[d] Dipartimento di Ingegneria, Università degli Studi di Palermo, Palermo, Italy
[e] Dipartimento DEIM, Università degli Studi della Tuscia, Viterbo, Italy
[f] Dipartimento DIBAF, Università degli Studi della Tuscia, Viterbo, Italy
[g] Water Management Department, Delft University of Technology, Delft, the Netherlands
[h] Metropolder Company, Rotterdam, the Netherlands
[i] Institute of Water & Environment, Florida International University, Miami, USA
*Corresponding author. E-mail: elena.cristiano@unica.it

EC, 0000-0002-0725-3014; AA, 0000-0001-6162-4691; CA, 0000-0003-3576-7052; DP, 0000-0002-4274-6316; SU, 0000-0003-4724-1998; FV, 0000-0003-1716-192X; RD, 0000-0001-5469-0199; RP, 0000-0003-1996-5921; AP, 0000-0003-4943-0928; FT, 0000-0002-5176-3492; AF, 0000-0001-7811-8023; FA, 0000-0001-8769-3812; LVN, 0000-0002-3280-2898; OH, 0000-0003-0676-3167; FN, 0000-0002-6562-3159

ABSTRACT

Green roofs have been widely recognized as sustainable nature-based solutions to mitigate floods in urban areas, which, in the last decades, are increasing due to the combination of intense worldwide urbanization and climate change. Besides flood mitigation, green roofs provide additional benefits for the urban environment (e.g., reducing the urban heat island and ensuring energy saving for the underneath building). Moreover, green roofs facilitate the increase of urban biodiversity, attracting different species of small animals, and upgrade the city aesthetic value. Among the different types of green roofs, multilayer blue-green roofs present an additional layer to store water during rainfall events. As part of the Polder Roof field lab project, prototypes of multilayer blue-green roof developed by the Dutch company Metropolder were installed in four Italian cities: Cagliari, Palermo, Perugia, and Viterbo. The four prototypes and the experimental set up are described and the potential benefits of this innovative solution are discussed. Preliminary analyses, from December 2020 to December 2021, enable to estimate runoff reduction and thermal properties of multilayer blue-green roofs, underlying the high potential of this nature-based solution, which allows to retain most of the rainfall events and to mitigate the daily temperature variability.

Key words: green roofs, nature-based solutions, resilience, thermal insulation, water management

HIGHLIGHTS

- Description of multilayer blue-green roofs installed in four Italian cities.
- Analysis of the multilayer blue-green roof retention capacity.
- Analysis of the multilayer blue-green roof thermal insultation properties.

GRAPHICAL ABSTRACT

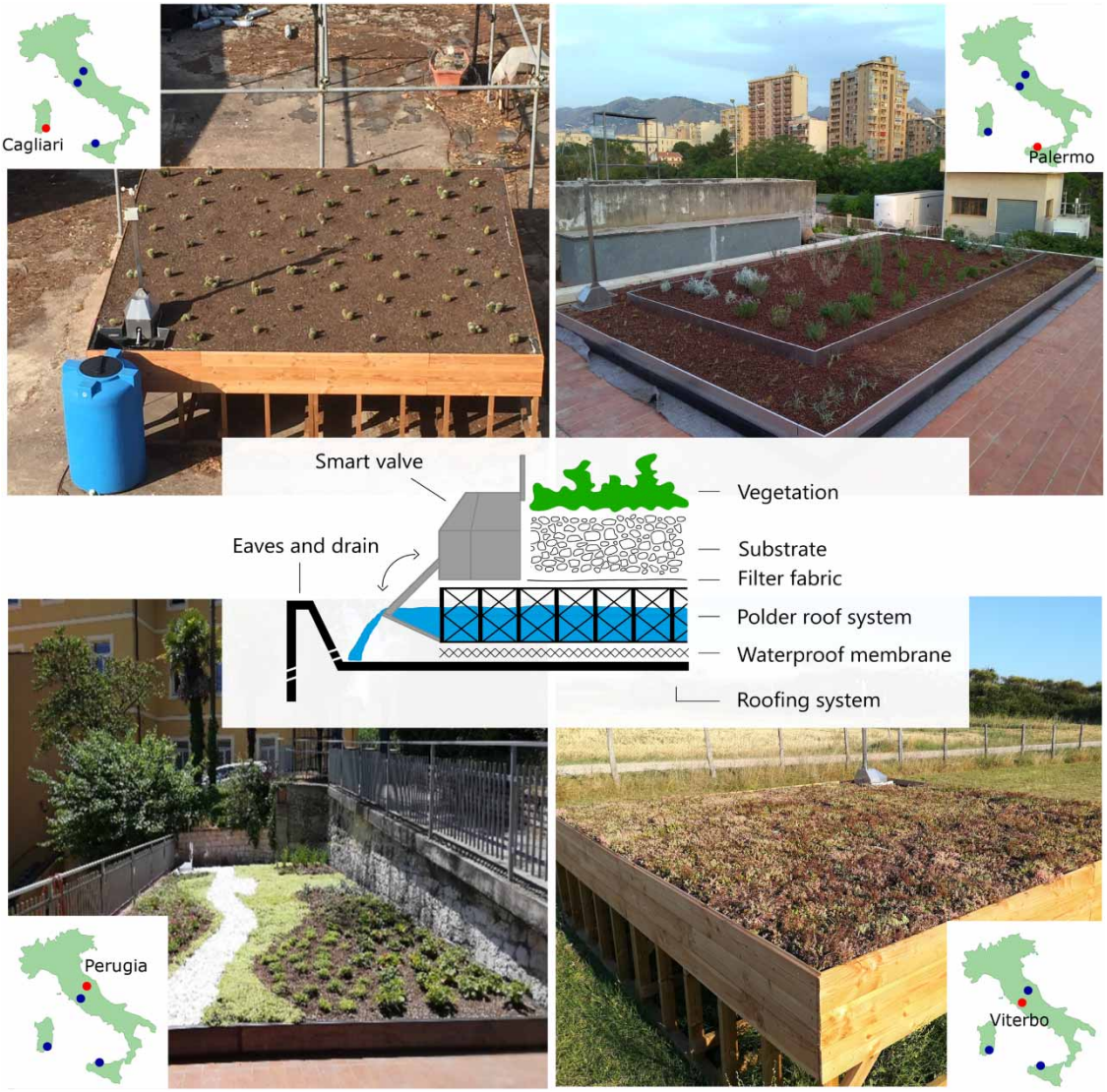

1. INTRODUCTION

Modern society is dealing with several challenges and global changes that are reshaping the urban environment. Population is growing fast and moving from rural to urban areas: projections show that the global population will reach 9.7 billion by 2050 and two-thirds of it will be living in cities (UN 2018), and a consequent increase in impermeabilization of natural surfaces is expected. At the same time, climate changes are expected to increase the global average temperature, with longer dry periods, alternated by short and highly intense rainfall events (IPCC 2007; Masson-Delmotte *et al.* 2018) also in the Mediterranean region (Treppiedi *et al.* 2021). The interplay of climate and urbanization changes is projected to facilitate increased pluvial flood generation and intensify urban heat islands (Arnone *et al.* 2018). Moreover, the COVID-19 pandemic and the consequent socio-economic crisis are strongly influencing and reshaping the way of thinking and living in the urban environment, and, in particular, the need for private green spaces is emerging (Hanzl 2020; Honey-Rosés *et al.* 2020; Jenkins 2020; Xie *et al.* 2020; Pelorosso *et al.* 2021a).

Different solutions have been proposed to mitigate and adapt to climate changes and population densification, creating smart, sustainable, and resilient cities, aiming to achieve the Sustainable Development Goals (SDGs) proposed in the Sustainable Agenda 2030. A solution to cope with urban rainwater excess is represented by rainwater harvesting systems. Such systems have been developed through the centuries in Mediterranean areas to collect and store water during rainfall

events, making it available during drought periods (Beckers *et al.* 2013). Besides this potential usage, rainwater harvesting systems are nowadays mainly used to mitigate extreme rainfall events (Boers & Ben-Asher 1982; Zhang & Hu 2014; Teston *et al.* 2018; Freni & Liuzzo 2019; Akter *et al.* 2020; Cristiano *et al.* 2021b). Thanks to their water storage capacity, rainwater harvesting tanks can reduce the pressure on the drainage systems, detaining a fraction of the rainfall during the events and releasing it in a later moment (Bocanegra-Martínez *et al.* 2014; Chao-Hsien *et al.* 2014; Sample & Liu 2014; Akter & Ahmed 2015; Campisano & Modica 2015; Campisano & Lupia 2017; Adugna *et al.* 2018; Cipolla *et al.* 2018; Abas & Mahlia 2019; Palermo *et al.* 2020). If properly stored and treated, this water can be reused for different domestic purposes, such as home-garden irrigation and flushing toilets, potentially reducing potable water consumption.

Besides these traditional solutions, which are often costly and not flexible, other engineering solutions, known as nature-based solutions (NBSs), have also been investigated to mitigate the impact of pluvial floods and to increase urban resilience to climate and demographic changes (Pelorosso *et al.* 2018; Oral *et al.* 2020; Recanatesi & Petroselli 2020; Calheiros & Stefanakis 2021). NBSs (e.g., green roofs (GRs), rainwater collection parks, permeable pavements, and wetlands) are solutions inspired and supported by nature that can provide multiple environmental, social, and economic benefits (i.e., ecosystem services) through locally adapted, resource-efficient, and systemic interventions (Faivre *et al.* 2017; Nesshöver *et al.* 2017; Oral *et al.* 2020). Among the different NBSs, GRs are one of the most important technologies to deal with the urban challenges. They have been mainly investigated for their capacity to mitigate pluvial floods, retaining a fraction of the rainfall event (Getter *et al.* 2007; Brandão *et al.* 2017; Cristiano *et al.* 2020, 2021a; Liu *et al.* 2020), and to thermal insulate the buildings, reducing the energy consumption (Lazzarin *et al.* 2005; Castleton *et al.* 2010; Coma *et al.* 2016). Moreover, GRs present multiple benefits: they guarantee biodiversity, help lowering the urban temperature and reducing the urban heat island (Takebayashi & Moriyama 2007; Susca *et al.* 2011; Santamouris 2014; Muhammad & Reeho 2017; Solcerova *et al.* 2017), retain contaminants in the soil layer, contribute to the CO_2 sequestration (Yang *et al.* 2008; Gregoire & Clausen 2011; Rowe 2011; Speak *et al.* 2012; Abhijith *et al.* 2017), and add aesthetic values to urban environments (van den Bosch & Ode Sang 2017; Kumar *et al.* 2019).

Multilayer blue-green roof (MGR) is an innovative technology that combines all the potential benefits of traditional GRs with the large storage capacity of rainwater harvesting systems (Shafique *et al.* 2016a, 2016b; Muhammad & Reeho 2017; Andenæs *et al.* 2018; Cristiano *et al.* 2021a). Compared to traditional GRs, this technology presents an additional layer below the soil layer, which can store the water leaked from the soil, thus, when the soil moisture reaches the leakage triggering point, water starts to percolate and is collected in the storage layer. The water level within the storage layer can be regulated by means of a remotely controlled valve, which can be also opened or closed manually if necessary.

As part of the Polder Roof field lab, a project supported by the European Climate-KIC programme, four MGR prototypes, called Polder Roofs and developed by the Dutch company Metropolder, have been installed in four Italian cities (Cagliari, Palermo, Perugia, and Viterbo) during Spring 2019, with the aim of exploring the potential benefits of this tool in Mediterranean climate regions. This work has the goal to present some preliminary results obtained during the first period of observation, comparing the potential of the four prototypes, which differ for their setup and installation properties (e.g., soil and vegetation type) and are influenced by different climatological conditions. Two specific benefits of the MGR installation are here investigated: the flood mitigation capacity and the thermal insulation.

The paper is structured as follows. Section 2 provides a general presentation of the MGR system proposed by the Metropolder company, with a detailed description of the four MGRs installed in Italy, focusing on the different characteristics that could influence the MGR retention capacity and temperature mitigation. Moreover, this section illustrates all the installed sensors and the observed data available for each study case. The methodology followed to assess preliminary analysis to evaluate the potential runoff mitigation capacity and thermal insulation potential of this tool are presented in Section 3, while results are illustrated in Section 4. Section 5 presents the potential benefits of MGR, discussing the role of the gate in the outflow generation and how this element can improve the urban drainage management compared to traditional GR. This section also includes an overview of the future research directions. Section 6, finally, summarizes the key points of the project and highlights the main conclusions of this preliminary analysis.

2. MGRS AND DESCRIPTION OF THE CASE STUDIES

2.1. Polder Roof by Metropolder: the blue-green roof technology

The Polder Roof is an innovative system at a Technical Readiness Level (TRL) of 7, designed by the Metropolder Company, to maximize the water retention capacity of a roof. Currently, there are more than 25 functioning Polder Roof systems in the

Netherlands and many more at the engineering stage. The system buffers and holds water while functioning as a foundation of an urban surface most commonly a GR, garden, or park. Though green is the current top layer, there is sustained interest in placing systems on hardened surfaces such as parking areas, streets, and pathways.

The Polder Roof structure is composed of multiple layers (Figure 1): from the top there is the vegetation, the soil substrate, a geotextile filter fabric to enable the water to flow holding the soil particles, a buffer where the water can be stored and a waterproof membrane to protect the roof. The buffer is made of Permavoid, a modular interlocking polypropylene void former. The storage capacity of the Polder Roof can be regulated by a smart remotely controlled valve, which can be opened or closed depending on the user's needs (Busker *et al.* 2022). For example, as shown in Figure 1, respectively, the user could decide to open the valve when heavy rain is forecast (Figure 1(a)) and to keep it closed during sunny periods (Figure 1(b)), with the aim to use the stored water for irrigation.

Using Metropolder's patent pending Sm^rtMILL (Figure 1(c)), the Polder Roof functions as a dynamic water buffer. The Sm^rtMILL contains sensors which measure rainfall, temperature, water height, and wind speed. Based on the levels of each of these components, the water held on the roof can be maintained or released through a valve connected to the roof drain. The Sm^rtMILL transmits its data to a personal dashboard which displays real-time conditions and allows for remote adjustments. Remotely controlled, fine-grained management, and distribution of stored water is the Polder Roofs contribution to urban resilience. The Polder Roof fits building regulations, policy aims, and is easily applicable and well scalable. The innovations regarding urban flooding, building heating and cooling, insulation, groundwater infiltration, grey water re-use, and urban agriculture are what set the Polder Roof apart from any rooftop system seen before (van der Meulen 2019; Pelorosso *et al.* 2021b).

2.2. The four Italian case studies

In this section, the characteristics of the prototypes located in Cagliari, Palermo, Perugia, and Viterbo are described, with a particular focus on the peculiarities that could influence the water retention capacity and the thermal insulation properties of

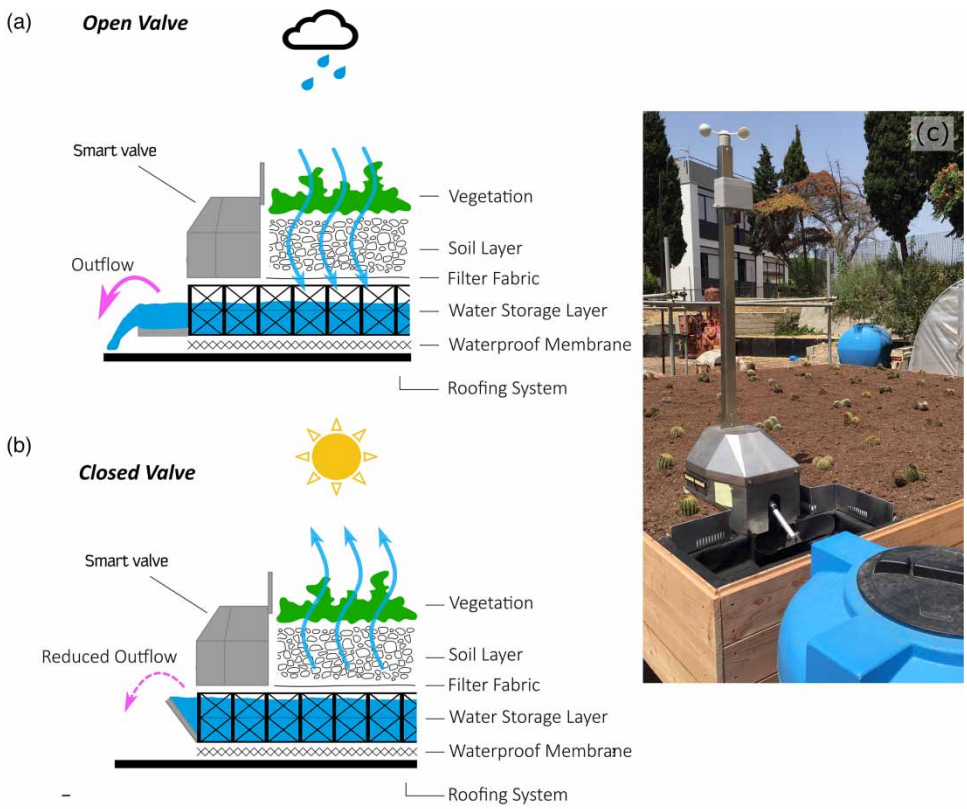

Figure 1 | The blue-green roof technology proposed by Metropolder. Schematization of the Polder Roof structure with a (a) open smart valve and (b) closed smart valve. (c) Example of the smart valve installed on the prototypes.

this system, such as soil and vegetation type. In some locations, the presence of a benchmark roof (either a bare roof or a traditional GR) will allow a comparison with the prototype to highlight the benefits of this innovative system. For each test case, Table 1 resumes the main characteristics of the system, the installed sensors, and the climate of the site where it is installed (e.g., mean annual rainfall depth and temperature reference values, derived from local historical time series).

The four Italian Polder Roofs are equipped with a standard monitoring station, which provides the real-time observation of essential climatic variables, and additional local instrumentation to pursue specific objectives of each case study. In particular, the standard Polder Roof monitoring station includes a tipping-bucket rain gauge, two thermometers for air and water temperature, an anemometer, and a sensor to monitor water level in the storage layer. The Metropolder monitoring station is connected to an online platform, which enables to easily read the different measurements and to regulate the water level in the storage layer, varying the opening degree of the valve.

To measure the runoff generation from the MGR, the outflow from the storage layer is directed into a rain barrel. A Baro-Diver® produced by the Van Essen Instruments company is placed in the rain barrel to measure the variation of pressure and, consequently, the water level. The temporal resolution of the water level measurements can be decided by the user: in Cagliari, for example, a time step of 1 min has been set, while in Palermo and Viterbo a 5-min time step is used. An external barometer allows compensating atmospheric pressure variations in real-time. Water heights are then converted into water volume by a specific calibration curve. The outflow from the MGR is then estimated by a mass conservation equation. Besides the described standard equipment, each Polder Roof has additional sensors that will be presented in the following sections. Figure 2(b)–2(e) illustrates the prototypes installed in the four case studies.

With the aim to better understand the differences among the case studies, Figure 2(a) shows the empirical complementary cumulative distribution function of the daily rainfall of historical time series in the four locations (circles) and the corresponding fit with a generalized Pareto distribution (thick lines), by the Multiple Threshold Method (Deidda 2010). Historical rainfall time series present different lengths for each case study: Cagliari (1947–1997), Palermo (2002–2020), Perugia (1990–2021), and Viterbo (1916–2015). The shape parameter k of the generalized Pareto distribution and the annual average rainfall m are reported in the legend of Figure 2(a). Higher values of the shape parameter k highlight a higher probability of observing extreme values with respect to the local average in the considered location.

2.2.1. MGR in Cagliari

The Polder Roof located in Cagliari (Figure 2(b)) is installed 50 cm above the ground on a wooden structure within the garden of the Department of Hydraulics and Hydrology of the Civil Engineering Faculty, University of Cagliari. The MGR has a surface of 16 m^2 (4 m $\times$ 4 m) and it is constituted by an 8 cm storage layer and an 8 cm of soil, classified as sand. The soil is planted with common cactus plants (*Cactaceae*), which represent one of the local species of the vegetation. These plants are characterized by a Crassulacean Acid Metabolism (CAM), that enables them to close the stoma during the day, avoiding water dispersion. The evapotranspiration efficiency of CAM vegetation is lower with respect to other plants, but it ensures the survival of the species even during very hot and dry periods. Moreover, CAM vegetation requires very low maintenance, with consequently low costs (Cristiano *et al.* 2020). For these reasons, this type of vegetation is particularly suitable for regions characterized by long hot and dry summers, such as the Mediterranean areas. The MGR outflow is directed into a 350-l rain barrel equipped with a Baro-Diver®.

In addition to the sensors included in the standard MGR monitoring station provided by Metropolder (see Sections 2.1 and 2.2), four thermometers (MX2203, produced by HOBO) have been installed to analyse the temperature in the soil, and beneath and on the wooden structure, on February 25, 2021. The four thermometers have been set to record the surface temperature with a 30-min resolution. Rainfall data have been provided by the Agency for the Environmental Protection of the Sardinia Region (Agenzia Regionale per la Protezione dell'Ambiente della Sardegna – ARPAS), which manages a dense rain gauge network in the region, with a weather station close to the prototype location. Rainfall data are available for the entire investigated period with a 1-min resolution.

2.2.2. MGR in Palermo

The MGR installed at the University of Palermo (Figure 2(c)) covers a rectangular area of about 32.0 m^2 (i.e., 4.30 m $\times$ 7.45 m) and is characterized by a green upper layer composed by two sub-areas with different depths; a central rectangular area, with an extension of about 18 m^2, is characterized by a soil thickness of 20 cm, while the remaining border region, whose extension is 14.0 m^2, has a shallower soil thickness of 10 cm. All sub-areas have been filled with a fertile soil consisting of a mixture of volcanic

Table 1 | Summary of the characteristics of the study cases

		Cagliari	Palermo	Perugia	Viterbo
Local climate characteristics	Average annual rainfall	425.3 mm/year	733.1 mm/year	896.4 mm/year	796.6 mm/year
	Average annual temperature	17.5 °C	17.0 °C	13.2 °C	14.4 °C
Polder Roof characteristics	Total surface	16 m^2 (4 m × 4 m)	32 m^2 (4.30 m × 7.45 m)	55 m^2 (11 m × 5 m)	16 m^2 (4 m × 4 m)
	Soil type	Common soil for Cactaceae, classified as *Sand* (granulometric analysis)	Volcanic materials (about 90% of volcanic lapillus and about 10% of pumice with a grain size of 0–10 mm)	Lightweight soil (40% pumice)	70% pumice, 20% peat, 10% sand
	Soil thickness	80 mm	1st area (14 m^2): 100 mm 2nd area (18 m^2): 200 mm	100 mm	100 mm
	Vegetation type	Cactus plants (*Cactaceae*)	1st area: mixture of sedum and meadow species: *Sedum album Stipa capensis, etc.* 2nd area: mixture of shrub species: *rosmarinus officinalis, teucrium fruticans, teucrium flavum, etc.*	*Sedum, Frankincense (Plectranthus), Aloe Vera, Delospermum*	*Sedum album, Sedum acre*
	Storage layer	80 mm	80 mm	80 mm	80 mm
Measurement tools	Rainfall	Metropolder station, from October 2019, with some gaps + ARPAS rain gauge close to the University (long historical data)	Metropolder station, from June 2019, with some gaps + disdrometer, weighing rain gauge, weather station equipped with a tipping rain gauge very close to the Polder Roof (~ 65 m).	Metropolder station, from October 2019, with some gaps + Official pluviometer from the Regional Hydrographic Service (~1 km from the Polder Roof).	provided by Metropolder station, from July 2019, with several gaps. + Rain gauges in the experimental site (Grimaldi *et al.* 2018)
	Water level	Metropolder station, from October 2019, with some gaps	Metropolder station, from January 2021	Metropolder station, from October 2019, with some gaps	N/A
	Outflow	One Rain barrel (350 l) with Baro-Diver® for the water level since December 2020 ($\Delta t = 1$ min).	Two Rain barrels (2 × 1,000 l) with Baro-Diver® for the water level since December 2020 ($\Delta t = 5$ min)	A rain barrel will be placed soon	Two Rain barrels (2 × 1,000 l) with Baro-Diver® for the water level since October 2020 ($\Delta t = 5$ min) +two additional rain barrels (2 × 1,000 l) installed in November 2021

(*Continued.*)

Table 1 | Continued

		Cagliari	Palermo	Perugia	Viterbo
	Temperature	Four HOBO sensors since February 2021: 2 below the roof, 1 over the soil, 1 aside north facing on the wooden structure (Figure 4(a))	Four HOBO sensors since December 2020: 1 below and 1 above the unaltered roof, 1 below the Polder Roof, 1 in the soil (~5 cm below the surface) (Figure 4(b)) 1 Lambrecht 8096 thermo-hygrometer sensor to measure the air temperature 2 m above the prototype	Three HOBO sensors installed on February 2020: 1 in the substrate not far from the Sm^rtMILL, 1 under the substrate between the plastic crates, 1 under the roof inside the carpentry (Figure 4(c))	Two HOBO sensors since November 2020: 1 above the Polder Roof and 1 above the benchmark. (Figure 4(d)) 2 additional HOBO thermometers (1 inside and 1 below the Polder Roof) could be included in future monitoring.
Investigated daily events	Number	13 (3 dry season–10 wet season)	50 (9 dry season–41 wet season)	18 (10 dry season–8 wet season)	37 (13 dry season–24 wet season)
	Mean intensity	21.7 mm (11.7 mm dry season–28.0 mm wet season)	14.7 mm (14.8 dry season–14.6 mm wet season)	15.4 mm (20.1 dry season–8.11 wet season)	13.0 mm (12.4 mm dry season–13.3 mm wet season)
	Max intensity	100.8 mm (22.6 mm dry season–100.8 mm wet season)	42.3 mm (42.3 mm dry season–40.6 wet season)	40 mm (40 mm dry season–10.8 mm wet season)	39.4 mm (13.7 dry season–39.4 mm wet season)
Additional notes		Soil moisture sensors have been installed in June 2021	Soil moisture sensors + Eddy Covariance Tower + further temperature sensors will be installed	Soil moisture sensors will be installed	Soil moisture sensors will be installed

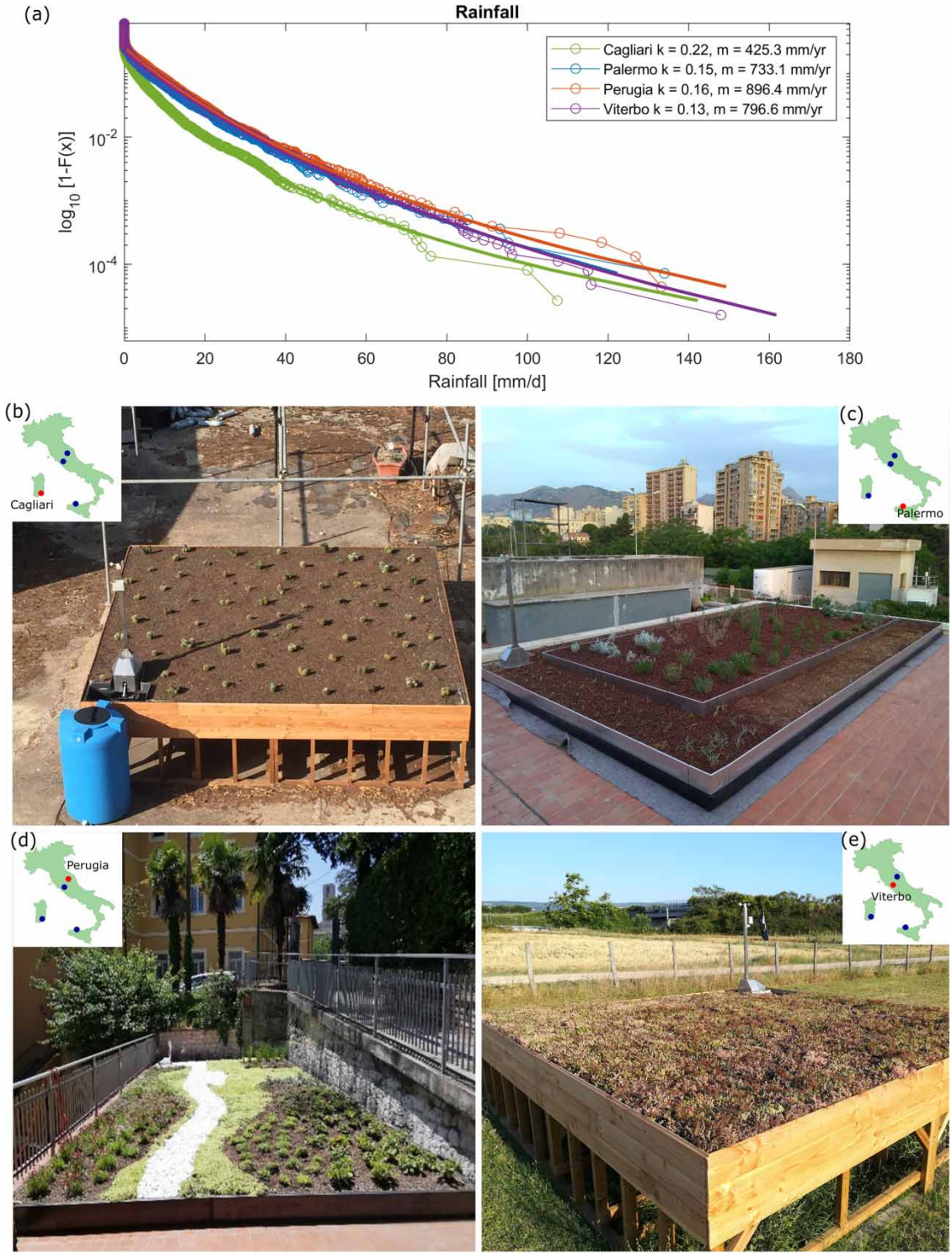

Figure 2 | Case studies. (a) Probability distribution of the daily rainfall. Polder Roof prototypes located in (b) Cagliari, (c) Palermo, (d) Perugia, and (e) Viterbo with the geographic location in the upper left corners.

materials (about 90% of volcanic lapillus and about 10% of pumice with a grain size of 0–10 mm). In order to facilitate vegetation growth, a combination of CAM plants and typical local species were selected. More specifically, the first area was installed with a system of shrub species of garrigue and herbaceous species, such as *Rosmarinus officinalis*, *Teucrium fruticans*, *Teucrium flavum*,

Pallenis maritima, *Helichrysum rupestre*, *Trifolium fragiferum*, *Lavandula spica*, *Crithmum maritimum*, *Micromeria graeca*, *Coridothymus capitatus*, *Dianthus ruipicola*, *Origanum heracleoticum*, and *Convolvulus cneorum*. The second area, instead, was realized with a mixture of sedum species and typical Mediterranean meadow species, such as *Sedum album, Sedum dasiphyllum, Sedum sediforme, Sedum anopetalum, Stipa capensis*, *Trifolium angustifolium*, *Trifolium stellatum*, *Aegylops geniculata*, *Silene coeli-rosa*. An almost equal size (36.8 m^2) bare roof area bordering the MGR installation is also monitored for comparison and it is referred to as 'unaltered roof'. Analogously to the installation of Cagliari, a system of two 1,000-l rain barrels and two Baro-Diver® pressure sensors allow to collect and compare the rainwater coming from the MGR and the unaltered roof.

Besides the observations provided by the standard MGR monitoring station (see Sections 2.1 and 2.2), additional data are collected from a weighing rain gauge (OTT Pluvio2-400), a disdrometer (OTT-Parsivel2), and a weather monitoring station equipped with a tipping-bucket rain gauge (DQA130.1 by LSI LASTEM), a thermo-hygrometer sensor (Lambrecht 8096) for the measurement of air temperature and relative humidity, an air pressure sensor (Lambrecht 8128), a global solar radiation sensor (Lambrecht 16131.3), and an ultrasonic wind speed and direction sensor (VENTUS-UBM by Lufft). All the instruments are approximately 65 m from the MGR. Finally, four thermometers (MX2203 HOBO) have been installed, with a couple of sensors placed on both the MGR and the unaltered roof surfaces, and inside the building, in correspondence of the MGR and the unaltered roof.

2.2.3. MGR in Perugia

The MGR in Perugia (Figure 2(d)) is placed on the top of the carpentry of the University for Foreigners of Perugia (Palazzina Orvieto, Perugia). The prototype is 55 m^2 wide and it is constituted by a 10 cm layer of lightened soil (40% pumice) to reduce the weight on the carpentry attic. Different types of plants are included, such as *Sedum, Frankincense (Plectranthus), Aloe Vera, Delospermum*. These plants can resist long dry periods without the need of any water supplies for irrigation in the summer months. The roof has a pathway with white pebbles for recreational activities. The installation of a 1,000-l barrel equipped with a pressure measurement to estimate the water level is in progress.

In addition to the measurement recorded by the standard MGR monitoring station (see Sections 2.1 and 2.2), three temperature sensors (MX2203 HOBO) have been placed, two in the soil layer and one under the roof, inside the carpentry. The temporal frequency of the measurements has been set equal to 5 min.

2.2.4. MGR in Viterbo

The MGR located in Viterbo (Figure 2(e)) presents a structure similar to the prototype of Cagliari. The MGR is located in the hydrological experimental site (www.mechydrolab.org) of Tuscia University. It is placed on top of a wooden structure, 90 cm above the ground, and has a total surface of 16 m^2 (4 m × 4 m). It is formed by an 8 cm height storage layer and 10 cm of soil. The vegetation is characterized by perennial camephytic plants adapted to survive in arid climates (*S. album* and *S. acre*). The MGR outflow is directed into a 1,000-l rain barrel equipped with a Baro-Diver®. A second 16 m^2 bare area, representing a benchmark steel roof, was installed a few meters far from the MGR and is monitored for comparison with another 1,000-l rain barrel and Baro-Diver® sensor. Two additional 1,000-l rain barrels have been installed in November 2021 to increase the time between two emptying and to reduce the risk of overflow in case of intense precipitation.

Besides the standard MGR monitoring station (see Sections 2.1 and 2.2), the climatic variables are monitored by additional sensors in the nearby Macroraingauge experimental installation (Grimaldi *et al.* 2018): four additional rain gauges, one thermometer for standard air temperature (placed in a shaded area), one pyranometer, and one additional anemometer are present. Two thermometers (HOBO) measure the temperatures just above the MGR and the benchmark roof. Two additional thermometers (MX2203 HOBO) have been placed on November 9, 2020 to measure the temperature above the MGR and the benchmark roof, with a time step of 5 min.

3. METHODOLOGY

Among the multiple benefits of the MGR installation on buildings, this study focuses on the potential effects of the MGR prototypes on the runoff generation reduction and their thermal insulation properties. With this aim, this section introduces quantitative indices to evaluate the performances of MGR in terms of water and temperature control.

3.1. Runoff reduction

Thanks to the soil and storage layers, the MGR can retain and store rainwater, thus reducing the runoff generation and consequently contributing to mitigate the pluvial flood risk. The MGR runoff reduction performances have been evaluated

through two indices which have been applied at the daily scale, with the aim to evaluate the retention capacity of both the soil layer and the system as a whole.

The first index is the MGR Index of retention R_{MGR}, which is defined as:

$$R_{MGR,i} = 1 - \frac{O_i}{P_i} \tag{1}$$

where O_i and P_i are the depths of daily outflow from the MGR and of daily rainfall at the ith day, respectively. $R_{MGR,i}$ can range between 0, when soil is saturated and storage layer is full and, consequently, no rainwater is retained, and 1, when there is no outflow generation. This index enables to evaluate the retention capacity of the entire MGR structure, but it does not allow to identify whether the rainfall is stored in the soil layer or in the storage layer.

The second index proposed in this study is the GR index of retention R_{GR}, which has been introduced to evaluate the retention capacity of only the soil layer component of the MGR and can be calculated as:

$$R_{GR,i} = 1 - \frac{\Delta h_i + O_i}{P_i} \tag{2}$$

where Δh_i is the daily difference of water level in the storage layer. $R_{GR,i}$ can vary between 0, when the soil is already saturated and no rainwater is retained by the soil layer, and 1, when all the rainfall is stored in the soil layer. This index has been already used in the literature to estimate the retention capacity of traditional GRs (Viola *et al.* 2017; Hellies *et al.* 2018; Cristiano *et al.* 2021b). Both $R_{GR,i}$ and $R_{MGR,i}$ indices provide complementary information to properly describe the behaviour of a MGR.

Rainfall data are available for each location at high temporal resolution (ranging between 1 and 5 min depending on the case study) and for long time windows, covering the period December 2020–December 2021. Water level in the storage layer and outflow measurements, instead, are not available yet in some locations; for this reason, it was not possible to estimate both $R_{GR,i}$ and $R_{MGR,i}$ for all the four installations.

With the aim to investigate the retention capacity of the MGRs under critical conditions, light rainfall events have been excluded from this study. Following Alpert *et al.* (2002), that investigated the increase of extreme daily rainfall events in Mediterranean regions and identified rainfall thresholds, we defined as '*light*' an event with daily rainfall depth lower than 4 mm. Hence, only events with a daily rainfall intensity equal to or higher than 4 mm have been considered in this study to assess $R_{GR,i}$ and $R_{MGR,i}$. The main characteristics of the selected daily events used to estimate the retention capacity of the MGR in each case study are summarized in Table 1.

3.2. Thermal properties

MGRs help reducing the roof surface temperature contributing to the thermal insulation of the building. To investigate this potential benefit and to quantify the temperature mitigation, four indices, proposed by Bevilacqua *et al.* (2017), have been here used. As for the runoff mitigation, this investigation focuses on data available during the period from December 2020 to December 2021. Temperature data are recorded with a time step of 5 min (HOBO sensors in Perugia and Viterbo), 10 min (Metropolder sensors), and 30 min (HOBO sensors in Cagliari and Palermo), while the indices are evaluated at the daily scale.

The four indices compare the temperature T^G in a certain gauge G to the temperature T^* in a reference sensor, which is identified as 'reference' to represent the unaltered conditions, without the installation of the MGR. Since each prototype presents a unique configuration of the temperature sensor placement, in some cases different sensors have been chosen as a benchmark, depending on the scope of the analyses and on the peculiarities of the study case.

The first proposed index is the average daily surface temperature ratio $STR_{av,i}$ at the ith day, defined as the ratio between the average daily temperature $T^G_{av,i}$ recorded at the selected gauge G and the average daily temperature $T^*_{av,i}$ observed by the temperature sensor chosen as benchmark in the analysis:

$$STR_{av,i} = \frac{T^G_{av,i}}{T^*_{av,i}} \tag{3}$$

The $STR_{av,i}$ presents values higher than 1 when the selected location presents an average daily temperature higher than the benchmark and lower than 1 for the opposite situation. $STR_{av,i}$ values close to 1 highlight that there are no significant differences between the two observations.

The second index is the maximum daily surface temperature ratio $STR_{max,\,i}$, defined as:

$$STR_{max,\,i} = \frac{T^{G}_{max,i}}{T^{*}_{max,i}} \tag{4}$$

where $T^{*}_{max,i}$ and $T^{G}_{max,i}$ are the maximum temperatures observed during the ith day at the benchmark gauge and at the selected gauge G, respectively. Similar to the $STR_{av,i}$, $STR_{max,i}$ presents values close to 1 when the difference between the maximum temperature at the selected gauge and at the benchmark gauge is very small.

Following the same approach, the minimum daily surface temperature ratio $STR_{min,i}$ has been defined as:

$$STR_{min,i} = \frac{T^{G}_{min,i}}{T^{*}_{min,i}} \tag{5}$$

where $T^{*}_{min,i}$ and $T^{G}_{min,i}$ are the minimum temperatures during the ith day at the benchmark gauge and at the selected gauge G, respectively. This index has been estimated for the days with minimum daily temperature higher than zero.

The last index is the daily temperature excursion ratio TER_i, which is defined as:

$$TER_i = \frac{T^{G}_{max,i} - T^{G}_{min,i}}{T^{*}_{max,i} - T^{*}_{min,i}} \tag{6}$$

This last index evaluates the effects of the MGR installation on both minimum and maximum temperature, in terms of daily temperature excursion.

4. RESULTS

This section presents and discusses the results obtained from the analysis of the collected data in the four case studies for a 1-year period, from December 2020 to December 2021. The benefits of the MGRs are analysed and evaluated in terms of rainwater retention capacity and the thermal insulation properties, using the indexes introduced in Section 3.

4.1. Runoff mitigation

As explained in Section 3.1, the retention capacity is evaluated through two indices, the R_{MGR} and R_{GR}, only for significant daily rainfall events, with a mean intensity higher than 4 mm/day. Depending on the available measurements, for each location it was possible to estimate R_{MGR} and R_{GR} in order to investigate the retention capacity of the entire MGR and the soil layer, respectively. Rainfall, outflow, and water level data were recorded at different time resolutions and then aggregated and analysed at the daily scale.

In Cagliari, the periods between June 1, 2021 and August 1, 2021, and between October 1 and 30, 2021, have been excluded for this case study, due to sensors malfunctioning. Although the Baro-Diver installed in the rain barrel in Cagliari was not recording, no outflow has been observed during the investigated period. In Perugia, the rain barrel with the Baro-Diver is not recording data yet, and for this reason, also in this case, only the R_{GR} has been estimated and evaluated for events that did not generate runoff. Finally, for the MGRs located in Palermo and Viterbo it was possible to estimate the R_{MGR} for the entire year, while the R_{GR} has been evaluated until September 2021 for the case of Palermo and not analysed for the case of Viterbo, since the sensors that measure the water lever in the storage layer did not work properly over the entire year. The gate has been always kept closed during the investigated period, except for Cagliari, where it has been periodically open for maintenance during the dry periods.

4.1.1. Retention capacity

Results are illustrated in Figure 3, where the boxplots show the annual variability of the two investigated indices R_{GR} and R_{MGR} for the different cases (Figure 3(a) and 3(b), respectively). The solid line indicates the median value of the index, while the diamond represents the average.

As illustrated in Figure 3(a), Cagliari and Palermo present similar R_{GR}, with an average retention capacity of the soil layer of 0.46 and 0.42, respectively, suggesting that most of the investigated rainfall events are only partially retained by the soil layer,

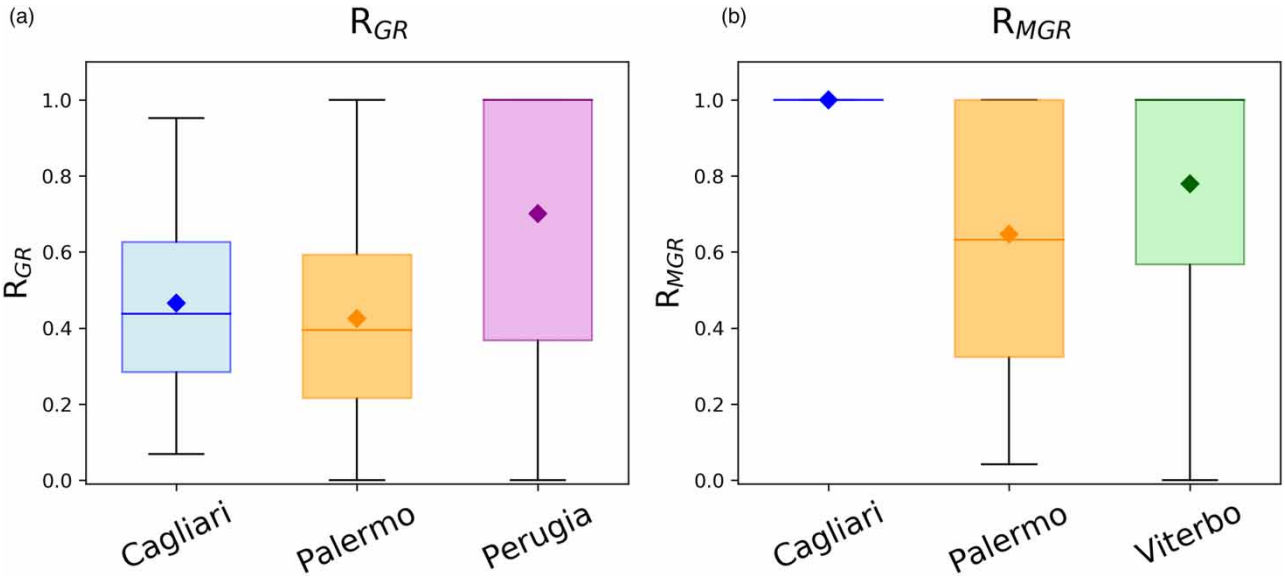

Figure 3 | R_{GR} (a) and R_{MGR} (b) estimated for the investigated locations. The solid line indicates the median value of the index, whereas the diamond represents its average.

and hence would have been only partially retained by a traditional GR, whose retention function is exclusively due to the soil layer retention capacity. The MGR of Perugia shows a higher performance in retaining the rainwater, probably due to the fact that, differently from the other two cases, it was not possible to measure the MGR outflow and, consequently, the events generating runoff, which usually are the most intense, has been excluded from the analysis.

The total retention capacity R_{MGR}, ensured by the MGR prototypes, can be observed in Figure 3(b) for the case study of Cagliari, Palermo, and Viterbo. Thanks to the contribution of the additional storage layer, the performance in this case is higher than the corresponding performance of a traditional GR, with an average R_{MGR} equal to 1 for Cagliari, to 0.65 for Palermo and to 0.75 for Viterbo. The plot shows that a significant number of rainfall events are completely retained by the systems, especially in Cagliari, where all events were fully retained, and in Viterbo, more than 50% of the events presented a R_{MGR} equal to 1.

In Palermo, the MGR retention capacity presents a high variability, with R_{MGR} mostly varying between 0.35 and 1. The high variability is determined by the different initial conditions that characterize the rainfall events. The antecedent conditions of soil water content and water level in the storage layer, in fact, strongly influence the retention capacity of a MGR.

The differences between the two indices, R_{MGR} and R_{GR}, and consequently the additional retention capacity provided by the storage layer in a MGR compared to a traditional GR, are well evident in the case of Palermo and Cagliari. In Palermo, when only the soil layer capacity is evaluated, the average R_{GR} is equal to 0.42, while, when the system as a whole is considered, the average index of retention R_{MGR} rises up to 0.65 and some of the events that were only partially retained by the soil layer, were instead fully retained by the entire system. In Cagliari, where the average annual rainfall depth is lower than in the other case studies (Table 1 and Figure 2), the MGR enabled to completely retain all the events, highlighting the high potential performance of the MGR installation in Mediterranean cities.

4.1.2. Seasonality effects

Results presented in this section show the seasonal performance of the MGRs, analysing separately the retention capacity during a warm and dry season, from March 22 to September 21, 2021, and a cold and rainy season, covering the complementary months of the year. The seasonal analysis emphasizes the high impact that antecedent soil moisture in the soil layer and water level in the storage layer have on the runoff mitigation.

The Spring-Summer rainfall events have been almost fully retained by the MGR in Palermo, with an average R_{MGR} equal to 0.87, and seven out of nine events completely retained by the structure. The two not fully retained events are consecutive and happened on March 22 and 23, 2021: in this case, the soil was already partially saturated and the storage layer partially full before the events, especially for the second day where conditions close to saturation were reached after the previous rainy day

and the R_{MGR} dropped to 0.3. In Viterbo, all the 13 Spring-Summer events have been fully retained by the MGR, confirming the importance that this tool can have on the runoff generation reduction.

The retention capacity estimated during the Autumn-Winter period is quite lower compared to the Spring-Summer seasons, due to the higher frequency and intensity of the rainfall events: the average R_{MGR} drops to 0.59 in Palermo and to 0.65 in Viterbo. Moreover, the temperature that characterizes this season is consistently lower than in the Spring-Summer period, limiting the evapotranspiration losses from the soil layer.

4.2. Thermal mitigation properties

This section analysed the potential thermal benefits that the installation of a MGR on a roof can provide, to contribute to the creation of a smart and resilient environment. The four thermal indices described in Section 3.2, are here estimated, and used to discuss the potential benefits of the installation of MGRs in terms of thermal impacts. For each location, multiple sensors have been installed in different points of the system, as illustrated in Figure 4.

In Cagliari, temperatures recorded from four gauges have been used to evaluate the potential thermal impacts of the MGR. The sensor position is schematized in Figure 4(a). Two types of sensors have been used for the analysis. The 'Air' sensor is provided by the Metropolder monitoring stations and refer to the air temperature above the wooden structure. Three HOBO sensor records have been investigated: one is installed few centimetres beneath the soil surface ('Soil'), and other two sensors are situated beneath the prototype, at diagonally-opposite corners ('Under1' and 'Under2'). The two sensors situated beneath the prototype are used to help understand the effects on the hypothetical underneath building. An average of the two-time series is plotted in Figure 4(e). The temperature time series for the Cagliari case study are available from February 25th to December 21, 2021 and are plotted in Figure 4(e).

Four HOBO temperature sensors have been installed in Palermo to evaluate the thermal insulation properties of the MGR, as illustrated in Figure 4(b). One sensor has been placed in the soil layer ('Soil'), a few centimetres below the surface, one has been located on the 'Unaltered Roof' surface, and other two sensors have been situated inside the building: one in correspondence of the MGR sensor ('Room1'), and the other one in correspondence of the 'Unaltered Roof' ('Room2'). Moreover, a Lambrecht 8096 thermo-hygrometer sensor is set to measure the air temperature 2 m above the roof ('Air'). In Palermo, temperature observations are available from December 2020 to December 2021 and are plotted in Figure 4(f).

In Perugia, temperature measurements from three gages are available: the 'Air temperature', provided by the Metropolder monitoring stations and other two HOBO sensors placed at 5 cm under the substrate, under the substrate lean on the plastic crate. In Perugia, the temperature time series are available from August 2021 and are illustrated in Figure 4(g).

Measurements from the two HOBO sensors have been evaluated in Viterbo for the entire 2021 and are presented in Figure 4(h). As schematized in Figure 4(d), one sensor has been set to measure the air temperature ('Air'), while the other two gauges have been installed in the soil layer of the MGR ('Soil') and on the unaltered roof ('Unaltered Roof'). In this way, it was possible to estimate the impact of the MGR installation on the surface temperature.

Although a direct comparison among all the case studies is not possible due to differences that characterize each location, some representative analyses may illustrate the thermal behaviour of a MGR and its thermal impact.

4.2.1. MGR vs unaltered roof

In order to investigate the thermal properties of a MGR, the first step is to compare the soil temperature with benchmark values referring to an unaltered roof. For this purpose, in Palermo and in Viterbo, a temperature sensor has been installed on an unaltered roof close by the MGR prototype (see Figure 4(b) and 4(d)). The four indices, proposed in Section 3.2, are here used to facilitate the visualization of the MGR thermal properties, comparing the soil temperature with the surface temperature of the unaltered roof. Figure 5(a) investigates the differences in the average daily temperature through the index STR_{av}, and it shows that on average the MGR daily temperature is 5–7% lower than the surface temperature of the unaltered roof for both the cases.

When comparing the differences in the minimum daily temperatures through the STR_{min} (Figure 5(b)), the MGR temperature is overall higher than the unaltered roof performance, suggesting that the prototype can ensure a good thermal inertia, increasing minimum temperature usually occurring during the night. In Palermo, for example, the MGR temperature is on average 40% higher than the unaltered roof temperature.

Following the same approach with the STR_{max}, plotted in Figure 5(c), it is clear that, in most of the cases, the presence of the MGR provides a benefit for the peak, usually diurnal, daily surface temperature, since the MGR temperature is lower than the

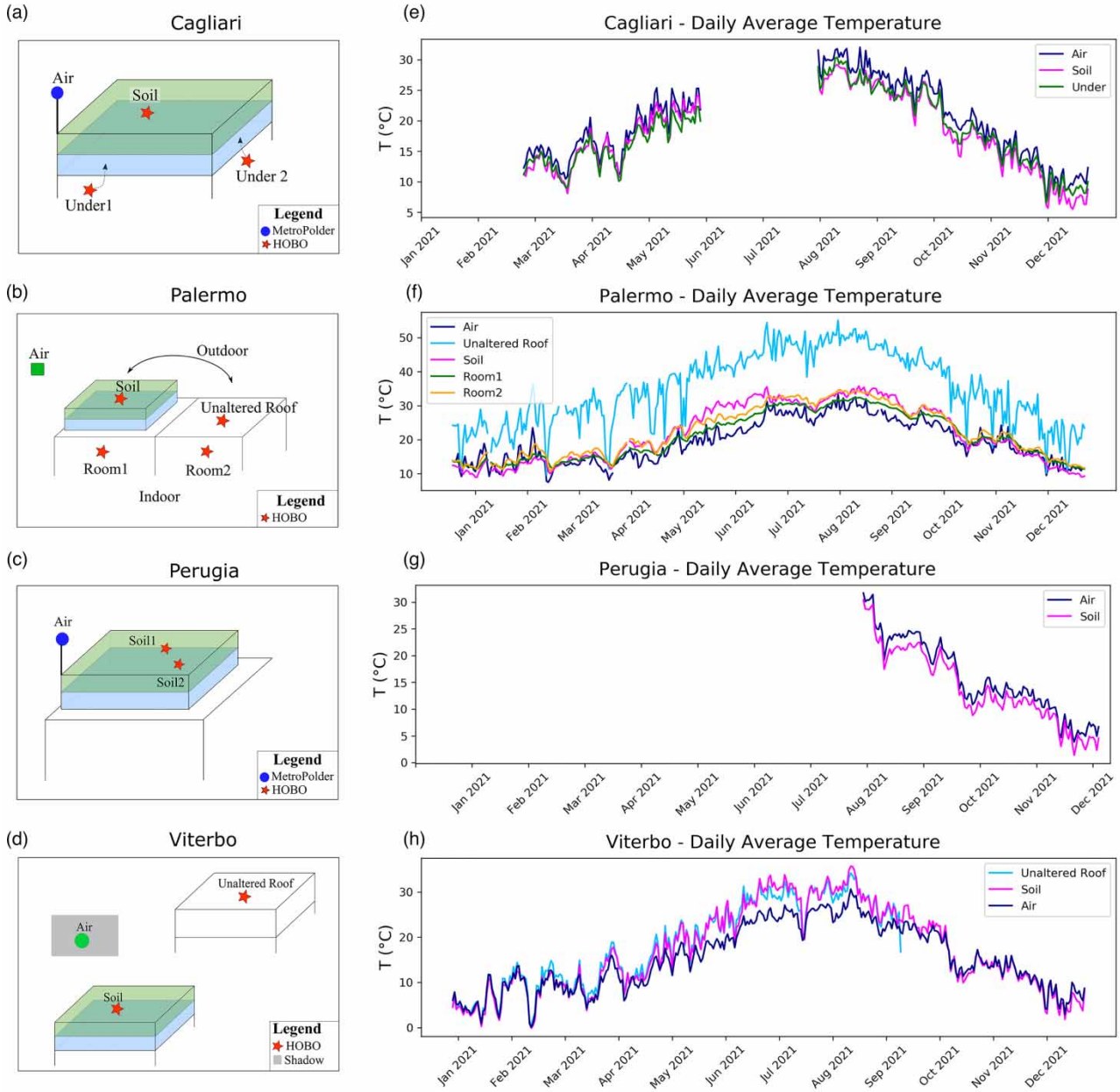

Figure 4 | Schematization of the MGR structure with the locations of the installed temperature sensors for each case study: (a) Cagliari, (b) Palermo, (c) Perugia and (d) Viterbo and related daily average temperature time series (e–h).

unaltered roof temperature. The effects are stronger in Palermo, where the daily peak air temperature, especially during the Summer, are usually higher than in Viterbo and, in fact, the maximum daily temperature on the MGR is on average reduced by about 40% compared to the corresponding unaltered values, while in Viterbo the average reduction is about 10%.

Finally, the variability of the TER, which describes the thermal excursion of the MGR with respect to that of the Unaltered Roof, is plotted in Figure 5(d). In both locations, the MGR shows a lower daily thermal excursion than the Unaltered Roof, with an average TER equal to 0.15 in Palermo and to 0.85 in Viterbo. Beyond the different climate conditions, the observed marked difference in performance between the two locations can be also addressed to the different materials of the Unaltered Roofs and the different vegetation coverage of the MGRs. Nevertheless, all the indices analysed here in both the case studies are concordant and highlight overall high performances of the MGR in mitigating the surface temperature of the roof,

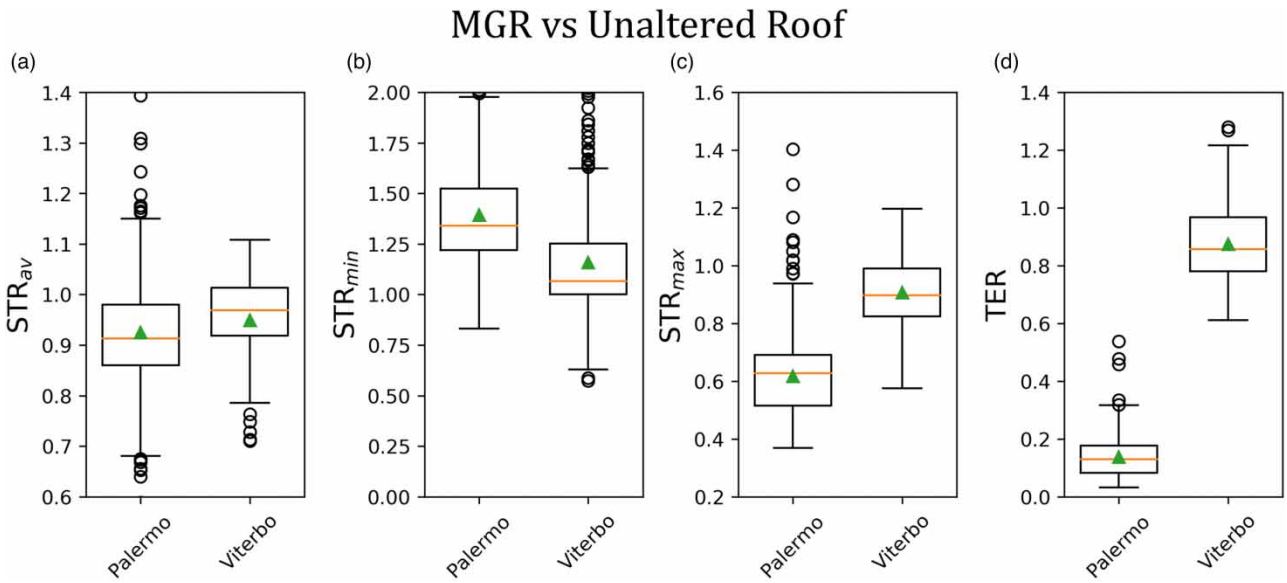

Figure 5 | Comparison between the MGR soil temperature and the surface temperature of the Unaltered Roof in Palermo and Viterbo. Boxplots for the indices (a) STR_{av}, (b) STR_{min}, (c) STR_{max}, and (d) *TER*.

suggesting an increased thermal inertia of the external surfaces, whose temperature results less influenced by the air temperature values and their daily excursions.

4.2.2. MGR and air temperature

The relationship between the surface temperature of a MGR and the air temperature is investigated through the four indices presented in Section 3.2, using the air temperature as the reference and the MGR soil temperature as the main gauge. Results are illustrated in Figure 6, where the boxplots represent the variability of STR_{av}, STR_{min}, STR_{max} and TER for the locations of Cagliari and Perugia.

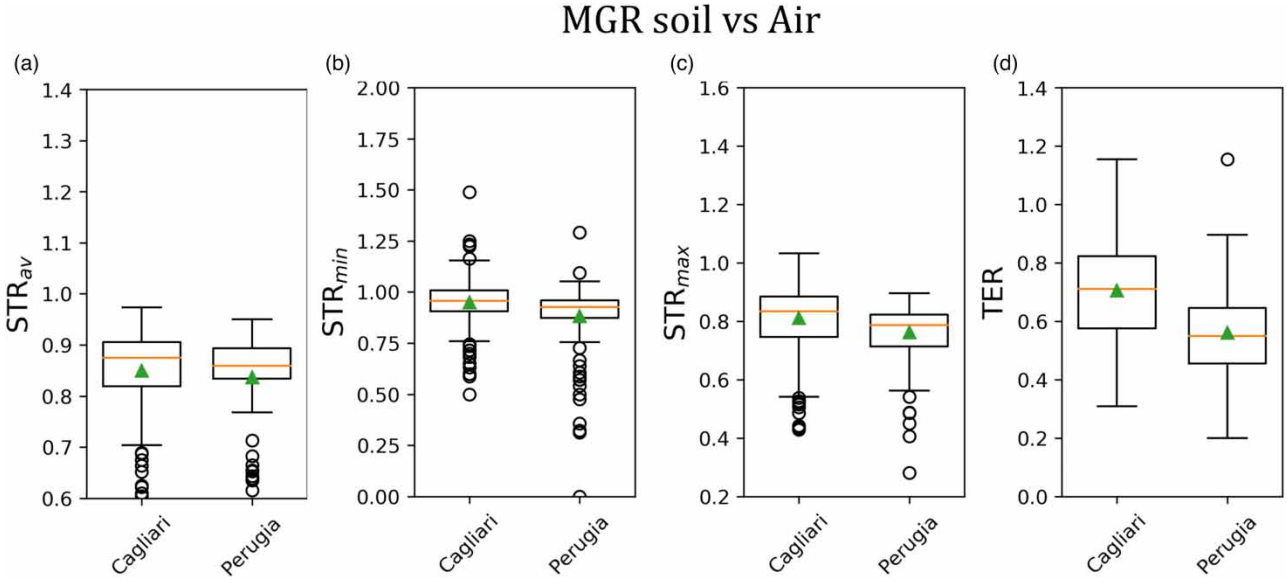

Figure 6 | Comparison between the MGR soil temperature and the air temperature in Cagliari and Perugia. Boxplots for the indices (a) STR_{av}, (b) STR_{min}, (c) STR_{max}, and (d) *TER*.

The STR_{av} analysis shows that the average MGR daily temperature is always lower than the air temperature, with an average reduction of about 15–20% (Figure 6(a)). The minimum and maximum daily temperatures for the MGR also presents overall values lower than the corresponding air temperature; more specifically, the differences between the minimum daily temperatures are rather low, with an average STR_{min} close to 1 in the Cagliari case study (Figure 6(b)), while a more significant lowering (on average reduction by the 20%) of the MGR temperatures compared to the air temperatures can be noticed for the maximum values (Figure 6(c)). More relevant differences can be observed between the daily thermal excursion of the MGR and the air (Figure 6(d)): the average TER is equal to 0.7 in Cagliari and to 0.55 in Perugia, confirming the high MGR capability to limit the daily temperature variability.

4.2.3. Potential thermal insulation for the building

The last analysis aims to directly investigate the thermal insulation properties of a MGR, comparing the temperature underneath the prototype with the soil temperature, used as reference value for the thermal indices. As shown in Figure 4, in the Cagliari case study, two HOBO temperature sensors have been placed beneath the prototype. The average between their measurements has been here used to derive the four thermal indices. In Palermo, a HOBO sensor has been installed inside the building, in correspondence with the prototype. Although the direct comparison between the two case studies is not possible, since in Palermo the roof structure influences the temperature inside the building, it is still possible to derive some conclusions regarding the thermal insulation properties of the MGR.

The STR_{av} varies around the unit, with average and median values over the entire observation period corresponding to about 1 year close to 1 for both locations (Figure 7(a)). However, analysing the values at seasonal scale (not reported in figure), it can be notice how STR_{av} assumes values above the unit prevalently during the Autumn-Winter season and below 1 during the Summer-Spring season, implying temperatures under the MGR (indoor for the case of Palermo) higher than the temperature on the soil surface during the colder period of the year and, on the contrary, lower temperature under the MGR during the hotter period, with a potential enhancement of the indoor internal comfort.

Different results can be achieved when investigating the minimum and maximum daily temperatures (Figure 7(b) and 7(c), respectively): in these cases, in fact, STR_{min} values prevalently higher than 1 and STR_{max} values lower than 1 over the entire 1-year period confirm that the temperature under the MGR is highly mitigated by the presence of the prototype itself. This can be inferred also by the analysis of the TER (Figure 7(d)), which reports for both location a thermal excursion under the MGR and inside the building constantly lower than that for soil surface of the MGR.

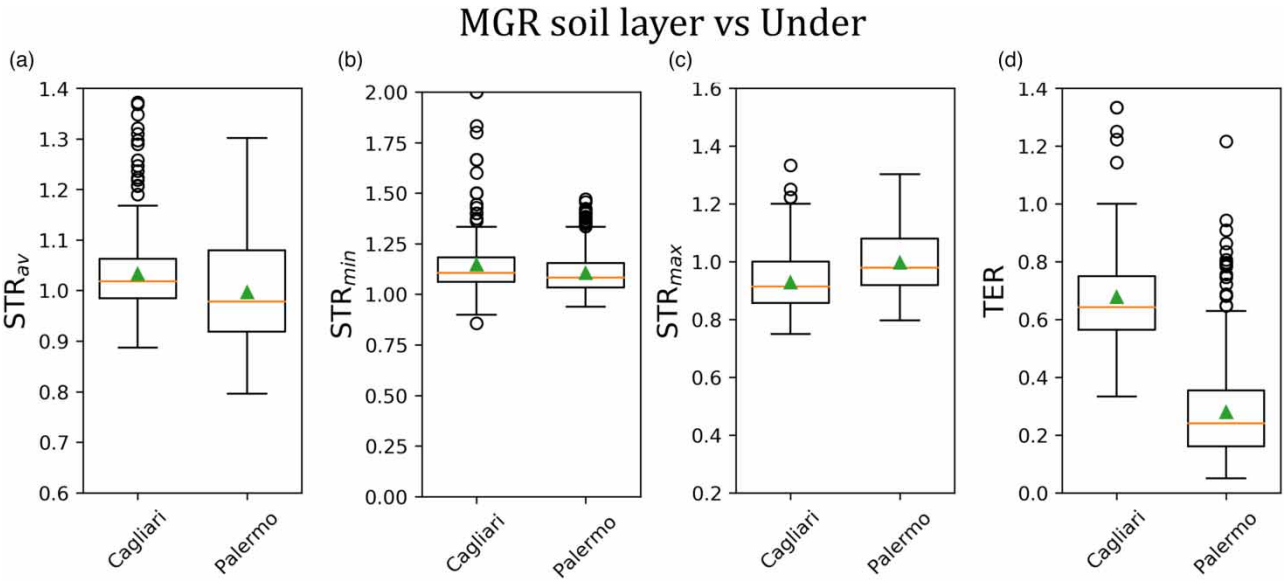

Figure 7 | Comparison between the MGR soil temperature and the temperature beneath the MGR structure in Cagliari and Palermo. Boxplots for the indices (a) STR_{av}, (b) STR_{min}, (c) STR_{max}, and (d) *TER*.

The roof configuration in Palermo enables to investigate the influence of the MGR on the temperature inside the building, comparing the recorded measures in Room 1, in correspondence of the prototype, and in Room 2, below the unaltered roof (see Figure 4(b) for the sensor configuration in Palermo and Figure 4(f) for the average daily time series). Daily temperatures in Room 1 are on average 1.3 °C lower than in Room 2 during the investigated period, while during the dry period, the difference increases up to a maximum of 3.7 °C. Moreover, the average TER between the temperatures recorded in Room 1 and in Room 2 mostly varies between 0.38 (25%-ile) and 0.95 (75%-ile), suggesting that the MGR contributes not only in reducing the average temperature inside the building, but also in limiting the daily excursion.

5. DISCUSSION

5.1. MGR performance

This study confirms the high potential of MGRs installed in Mediterranean areas in mitigating the runoff generation and in thermal insulating the underneath building. Traditional GRs guarantee an average rainfall reduction generally higher than the 50% of medium and intense rainfall events (Palla *et al.* 2010; Brandão *et al.* 2017; Palermo *et al.* 2019), with a strong variability connected to the structure features (such as soil type and thickness, vegetation type) and weather characteristics. These results have been confirmed by this study, where the analysis of the retention capacity guaranteed by the soil layer, represented by the R_{GR}, reported an average rainfall reduction between 42 and 70%, for the investigated case studies. Thanks to the additional layer, the MGRs ensure a higher volume to store rainwater, with an average retention index that reaches 0.65 in Palermo, 0.75 in Viterbo, and 1 in Cagliari.

These results support the findings presented by Busker *et al.* (2022), who investigated the hydrological performance of a MGR in the Netherlands. The different climatological environment leads to a different retention capacity, slightly lower in The Netherlands than in Mediterranean areas. As shown in Section 4, in fact, the retention and storage capacity of the MGRs installed in the Mediterranean areas enable to retain all the rainfall events in Spring-Summer. The high retention capacity in this case is facilitated by the low frequency of the events and by the high evapotranspiration rates, which ensures a higher probability that a rainfall event occurs when the soil is completely dry, and the storage layer is empty.

The retention capacity of the system, especially during the Autumn-Winter season, when rainfall events present higher intensity and frequency in Mediterranean areas, could be increased using a thicker storage layer. In many cases, this solution, however, might not be feasible, especially for already existing building, where the roof might not be able to sustain the weight of a large additional storage layer. An easier solution is given by a functional management of the gate that can optimize the water level in the storage layer, increasing the volume available to store rainwater.

Besides the high retention capacity, the preliminary analysis presented in this work, also emphasizes the additional benefits of a MGR, especially regarding thermal insulation. Compared to a traditional roof, the MGRs have shown lower maximum daily surface temperatures and higher minimum ones, and a lower thermal excursion during the day. These preliminary results suggest a high thermal insulation capacity for the underneath building, which can be translated in a potential save of energy for heating and cooling (Castleton *et al.* 2010; Coma *et al.* 2016).

5.2. The role of the gate to control the outflow

In this preliminary analysis, where the main goal was to present the potential benefits of the MGR prototypes under Mediterranean climate, the influence of the gate management has not been evaluated, since the gate was always closed. However, it cannot be ignored that the retention capacity and the thermal insulation properties of a MGR are strongly affected by the water level in the storage layer.

The retention capacity of a MGR can be largely increased through a wise management of the gate that regulates the water storage layer. As shown in Figure 1, the gate allows to regulate the water level in the blue layer, with the aim to accumulate rainfall and release it as runoff when it is more convenient, depending on the user's needs. If the main goal is to mitigate runoff, for example, the gate should be closed when it is raining, and the harvested water should be released when the rainfall event is over, and the urban drainage system is not stressed anymore. On the other hand, if there is the need to re-use the harvested water for irrigation or other domestic purposes, the gate should be kept closed, to accumulate a larger volume of water. It is therefore clear that, depending on the goals that need to be achieved with the MGR installation, a different management of the gate should be evaluated to optimize the benefits of the system. Busker *et al.* (2022) recently investigated the potential improvement of the retention capacity of a MGR very similar to those tested in this work, when integrating the gate management with the weather forecasts. This choice enables to empty the storage layer before intense rainfall events and

could largely reduce the peak runoff and increases the peak delay. The study calculates that the MGR in the Netherlands can reach a capture rate of 90% for total precipitation when using weather forecast to manage the gate opening. In arid and semi-arid climates, an optimized gate management can allow not only to mitigate the runoff generation, but also ensures water storage, that can be used, especially in Mediterranean cities, to limit additional irrigations and to reduce the pressure on the water supply system. Future analyses will be, hence, dedicated to understanding how the system may alter water quality to evaluate the potential reuses of water collected by the MGR for different purposes.

5.3. Urban scale MGR installation

Recently, Busker *et al.* (2022) assessed that converting all the potentially suitable roofs in Amsterdam to the MGR would determine 11% of extreme precipitation (>20 mm/hour) to be captured when using proper gate management with the weather forecasts. However, the different climate and typology of Mediterranean cities call for specific and local evaluations. Although the preliminary analysis presented in this work already highlights the potential benefits of MGRs as a sustainable solution for the development of the urban environment, further investigations need to be carried out to fully understand the behaviour of this innovative system in Mediterranean climate and to emphasize the potential impacts and benefits for society. From this point of view, an evaluation of the potential impacts of the MGR at the urban scale would be desirable, i.e., assuming the installation of this system over a great number of suitable roofs in a large neighbourhood or at city scale.

Future applied research will aim at implementing and testing modelling tools to identify best solution and localization of MGR for the mitigation of hydraulic risk and runoff reduction in performance-based planning and design contexts (La Rosa & Pappalardo 2020; Pelorosso 2020). An evaluation at the urban catchment scale will then allow flood mitigation capacity of NBS-based scenarios to be tested considering different costs and levels of interventions. Further analyses will be then dedicated to the definition of the criteria for the identification of potential buildings for the MGR retrofit and the creation of smart and resilient Mediterranean cities. Following this approach, it will also be possible to assess other ecosystem services, as the heat island attenuation or the pollution retention, for a more holistic evaluation of the MGR technology.

6. CONCLUSIONS

This work describes the installation of MGRs prototypes in four Italian cities (Cagliari, Palermo, Perugia, and Viterbo) as part of the Polder Roof field lab project. Compared to traditional GRs, MGRs present an additional water storage layer that increases the rainwater retention capacity of the system. The four installed prototypes are equipped with a standard monitoring station, provided by Metropolder, and differ for their setting, geometry and extension, vegetation and soil types, and some additional monitoring instruments. Moreover, although all cities are located in the Mediterranean area, each site is characterized by different climatological conditions. This work presents preliminary analyses that investigate the retention capacity and the thermal insulation properties of MGRs, comparing measurements and results from the four prototypes during the period from December 2020 to December 2021.

To estimate the rainwater retention capacity of this system, two indices have been proposed, focusing on the performance of the entire structure or only of the soil layer. Results show how the MGR structure ensures a retention capacity higher than a traditional GR and enables to retain most of the high-intensity rainfall events, especially in the warm season. This suggests the need for a weather-based optimization of the MGR gate to control water storage in the wet season for Mediterranean climate.

Four indices have been introduced to evaluate the potential implications of the MGR installation on the temperature of the surrounding environment and in the buildings underneath the multilayer roof. Since each site presents a peculiar configuration of the MGR and different locations of the temperature sensors, it was not possible to make a direct comparison among all study cases. However, in all locations it was possible to observe a positive impact of the MGR, which helps to mitigate the daily thermal excursion in all sites. The high potential of the MGR is clearly visible in the Palermo case study, where the daily temperature excursion of the room directly beneath the MGR is lower than that measured at the room beneath the unaltered roof.

On top of the exploratory hydrological and energetical analysis, this work offers a panoramic view of the future research outlines and directions that needs to be followed in order to fully understand the potential benefits of MGR in Mediterranean Climate. Further analysis will focus on the following:

- the implementation of an ecohydrological model for reproducing the MGR behaviour, from the soil moisture dynamics to the evapotranspiration and outflow;

- the optimal management practices for the gate control, to facilitate the regulation of the water storage, based on the specific purposes;
- the water quality of the MGR outflow, in order to evaluate possible re-uses and plan adequate treatments; and
- the assessment of the potential impact of the MGRs at the urban scale, identifying suitable locations for the NBS installation in each of the four cities.

ACKNOWLEDGEMENTS

Funding received from the European Union Climatic KIC programme with grant number EIT SGA 2018 supporting project 'Polder Roof Fieldlabs (180522)'. This work has also been partially funded by the Florisa Melone Award, promoted by the Italian Hydrological Society (IHS).

DATA AVAILABILITY STATEMENT

All relevant data are included in the paper or its Supplementary Information.

CONFLICT OF INTEREST

The authors declare there is no conflict.

REFERENCES

Abas, P. E. & Mahlia, T. 2019 Techno-economic and sensitivity analysis of rainwater harvesting system as alternative water source. *Sustainability* **11** (8), 2365.

Abhijith, K. V., Kumar, P., Gallagher, J., McNabola, A., Baldauf, R., Pilla, F., Broderick, B., Di Sabatino, S. & Pulvirenti, B. 2017 Air pollution abatement performances of green infrastructure in open road and built-up street canyon environments – a review. *Atmospheric Environment* **162**, 71–86. https://doi.org/10.1016/j.atmosenv.2017.05.014.

Adugna, D., Jensen, M. B., Lemma, B. & Gebrie, G. S. 2018 Assessing the potential for rooftop rainwater harvesting from large public institutions. *International Journal of Environmental Research and Public Health* **15** (2). doi:10.3390/ijerph15020336.

Akter, A. & Ahmed, S. 2015 Potentiality of rainwater harvesting for an urban community in Bangladesh. *Journal of Hydrology* **528**, 84–93. doi:10.1016/j.jhydrol.2015.06.017.

Akter, A., Tanim, A. H. & Islam, M. K. 2020 Possibilities of urban flood reduction through distributed-scale rainwater harvesting. *Water Science and Engineering* **13** (2), 95–105. https://doi.org/10.1016/j.wse.2020.06.001.

Alpert, A., Ben-Gai, T., Baharad, A., Benjamini, Y., Yekutieli, D., Colacino, M., Diodato, L., Ramis, C., Homar, V., Romero, R., Michaelides, S. & Manes, A. 2002 The paradoxical increase of Mediterranean extreme daily rainfall in spite of decrease in total values. *Geophysical Research Letters* **29** (11), 31-1–31-4. https://doi.org/10.1029/2001GL013554.

Andenæs, E., Kvande, T., Muthanna, T. M. & Lohne, J. 2018 Performance of blue-green roofs in cold climates: a scoping review. *Buildings* **8** (4), 55.

Arnone, E., Pumo, D., Francipane, A., La Loggia, G. & Noto, L. V. 2018 The role of urban growth, climate change, and their interplay in altering runoff extremes. *Hydrological Processes* **32** (12), 1755–1770.

Beckers, B., Berking, J. & Schütt, B. 2013 Ancient water harvesting methods in the drylands of the Mediterranean and Western Asia. *Journal for Ancient Studies* **2**, 145–164.

Bevilacqua, P., Mazzeo, D., Bruno, R. & Arcuri, N. 2017 Surface temperature analysis of an extensive green roof for the mitigation of urban heat island in southern mediterranean climate. *Energy and Buildings* **150**, 318–327. https://doi.org/10.1016/j.enbuild.2017.05.081.

Bocanegra-Martínez, A., Ponce-Ortega, J. M., Nápoles-Rivera, F., Serna-González, M., Castro-Montoya, A. J. & El-Halwagi, M. M. 2014 Optimal design of rainwater collecting systems for domestic use into a residential development. *Resources, Conservation and Recycling* **84**, 44–56. https://doi.org/10.1016/j.resconrec.2014.01.001.

Boers, T. M. & Ben-Asher, J. 1982 A review of rainwater harvesting. *Agricultural Water Management* **5** (2), 145–158. https://doi.org/10.1016/0378-3774(82)90003-8.

Brandão, C., Cameira, M. d. R., Valente, F., Cruz de Carvalho, R. & Paço, T. A. 2017 Wet season hydrological performance of green roofs using native species under Mediterranean climate. *Ecological Engineering* **102**, 596–611. https://doi.org/10.1016/j.ecoleng.2017.02.025.

Busker, T., de Moel, H., Haer, T., Schmeits, M., van den Hurk, B., Myers, K., Cirkel, D. G. & Aerts, J. 2022 Blue-green roofs with forecast-based operation to reduce the impact of weather extremes. *Journal of Environmental Management* **301**, 113750. DOI:https://doi.org/10.1016/j.jenvman.2021.113750.

Calheiros, C. S. C. & Stefanakis, A. I. 2021 Green roofs towards circular and resilient cities. *Circular Economy and Sustainability*. doi:10.1007/s43615-021-00033-0.

Campisano, A. & Lupia, F. 2017 A dimensionless approach for the urban-scale evaluation of domestic rainwater harvesting systems for toilet flushing and garden irrigation. *Urban Water Journal* **14** (9), 883–891. doi:10.1080/1573062X.2017.1279192.

Campisano, A. & Modica, C. 2015 Appropriate resolution timescale to evaluate water saving and retention potential of rainwater harvesting for toilet flushing in single houses. *Journal of Hydroinformatics* **17** (3), 331–346. doi:10.2166/hydro.2015.022.

Castleton, H. F., Stovin, V., Beck, S. B. M. & Davison, J. B. 2010 Green roofs; building energy savings and the potential for retrofit. *Energy and Buildings* **42** (10), 1582–1591. https://doi.org/10.1016/j.enbuild.2010.05.004.

Chao-Hsien, L., En-Hao, H. & Yie-Ru, C. 2014 Designing a rainwater harvesting system for urban green roof irrigation. *Water Supply* **15** (2), 271–277. doi:10.2166/ws.2014.107.

Cipolla, S. S., Altobelli, M. & Maglionico, M. 2018 Systems for rainwater harvesting and greywater reuse at the building scale: a modelling approach. *Environmental Engineering and Management Journal* **17** (10), 2349–2360.

Coma, J., Pérez, G., Solé, C., Castell, A. & Cabeza, L. F. 2016 Thermal assessment of extensive green roofs as passive tool for energy savings in buildings. *Renewable Energy* **85**, 1106–1115.

Cristiano, E., Urru, S., Farris, S., Ruggiu, D., Deidda, R. & Viola, F. 2020 Analysis of potential benefits on flood mitigation of a CAM green roof in Mediterranean urban areas. *Building and Environment* **183**, 107179. https://doi.org/10.1016/j.buildenv.2020.107179.

Cristiano, E., Deidda, R. & Viola, F. 2021a The role of green roofs in urban Water-Energy-Food-Ecosystem nexus: a review. *Science of The Total Environment* **756**, 143876. https://doi.org/10.1016/j.scitotenv.2020.143876.

Cristiano, E., Farris, S., Deidda, R. & Viola, F. 2021b Comparison of blue-green solutions for urban flood mitigation: a multi-city large-scale analysis. *PLOS ONE* **16** (1), e0246429. doi:10.1371/journal.pone.0246429.

Deidda, R. 2010 A multiple threshold method for fitting the generalized Pareto distribution to rainfall time series. *Hydrol. Earth Syst. Sci.* **14** (12), 2559–2575. doi:10.5194/hess-14-2559-2010.

Faivre, N., Fritz, M., Freitas, T., de Boissezon, B. & Vandewoestijne, S. 2017 Nature-based solutions in the EU: innovating with nature to address social, economic and environmental challenges. *Environmental Research* **159**, 509–518.

Freni, G. & Liuzzo, L. 2019 Effectiveness of rainwater harvesting systems for flood reduction in residential urban areas. *Water* **11** (7), 1389.

Getter, K. L., Rowe, D. B. & Andresen, J. A. 2007 Quantifying the effect of slope on extensive green roof stormwater retention. *Ecological Engineering* **31** (4), 225–231. https://doi.org/10.1016/j.ecoleng.2007.06.004.

Gregoire, B. G. & Clausen, J. C. 2011 Effect of a modular extensive green roof on stormwater runoff and water quality. *Ecological Engineering* **37** (6), 963–969. https://doi.org/10.1016/j.ecoleng.2011.02.004.

Grimaldi, S., Petroselli, A., Baldini, L. & Gorgucci, E. 2018 Description and preliminary results of a 100 square meter rain gauge. *Journal of Hydrology* **556**, 827–834.

Hanzl, M. 2020 Urban forms and green infrastructure – the implications for public health during the COVID-19 pandemic. *Cities & Health* 1–5. doi:10.1080/23748834.2020.1791441.

Hellies, M., Deidda, R. & Viola, F. 2018 Retention performances of green roofs worldwide at different time scales. *Land Degradation & Development* **29** (6), 1940–1952. doi:10.1002/ldr.2947.

Honey-Rosés, J., Anguelovski, I., Chireh, V. K., Daher, C., Konijnendijk van den Bosch, C., Litt, J. S., Mawani, V., McCall, M. K., Orellana, A., Oscilowicz, E., Sánchez, U., Senbel, M., Tan, X., Villagomez, E., Zapata, O. & Nieuwenhuijsen, M. J. 2020 The impact of COVID-19 on public space: an early review of the emerging questions – design, perceptions and inequities. *Cities & Health* 1–17. doi:10.1080/23748834.2020.1780074.

IPCC, I.P.o.C.C 2007 *Climate Change 2007: Impacts, Adaptation and Vulnerability. Contribution of Working Group II to the Fourth Assessment Report of the Intergovernmental Panel on Climate Change*. Cambridge University Press, Cambridge, UK, p. 976.

Jenkins, A. 2020 Biotic systems as a critical urban infrastructure during crisis: learning from the COVID-19 pandemic. *Cities & Health* 1–3. doi:10.1080/23748834.2020.1789821.

Kumar, P., Druckman, A., Gallagher, J., Gatersleben, B., Allison, S., Eisenman, T. S., Hoang, U., Hama, S., Tiwari, A., Sharma, A., Abhijith, K. V., Adlakha, D., McNabola, A., Astell-Burt, T., Feng, X., Skeldon, A. C., de Lusignan, S. & Morawska, L. 2019 The nexus between air pollution, green infrastructure and human health. *Environment International* **133**, 105181. https://doi.org/10.1016/j.envint.2019.105181.

La Rosa, D. & Pappalardo, V. 2020 Planning for spatial equity – a performance based approach for sustainable urban drainage systems. *Sustainable Cities and Society* **53**, 101885. https://doi.org/10.1016/j.scs.2019.101885.

Lazzarin, R. M., Castellotti, F. & Busato, F. 2005 Experimental measurements and numerical modelling of a green roof. *Energy and Buildings* **37** (12), 1260–1267. https://doi.org/10.1016/j.enbuild.2005.02.001.

Liu, L., Sun, L., Niu, J. & Riley, W. J. 2020 Modeling green roof potential to mitigate urban flooding in a Chinese city. *Water* **12** (8), 2082.

Masson-Delmotte, V., Zhai, P., Pörtner, H.-O., Roberts, D., Skea, J. & Shukla, P. R. (eds). 2018 Global warming of 1.5 C. An IPCC Special Report on the impacts of global warming. IPCC, Geneva, pp. 1-9. Available from: https://www.ipcc.ch/site/assets/uploads/sites/2/2019/06/SR15_Full_Report_Low_Res.pdf.

Muhammad, S. & Reeho, K. 2017 Application of green blue roof to mitigate heat island phenomena and resilient to climate change in urban areas: a case study from Seoul, Korea. *Journal of Water and Land Development* **33** (1), 165–170. https://doi.org/10.1515/jwld-2017-0032.

Nesshöver, C., Assmuth, T., Irvine, K. N., Rusch, G. M., Waylen, K. A., Delbaere, B., Haase, D., Jones-Walters, L., Keune, H., Kovacs, E., Krauze, K., Külvik, M., Rey, F., van Dijk, J., Vistad, O. I., Wilkinson, M. E. & Wittmer, H. 2017 The science, policy and practice of nature-based solutions: an interdisciplinary perspective. *Science of the Total Environment* **579**, 1215–1227. https://doi.org/10.1016/j.scitotenv.2016.11.106.

Oral, H. V., Carvalho, P., Gajewska, M., Ursino, N., Masi, F., van Hullebusch, E. D., Kazak, J. K., Exposito, A., Cipolletta, G., Raaschou Andersen, T., Finger, D. C., Simperler, L., Regelsberger, M., Rous, V., Radinja, M., Buttiglieri, G., Krzeminski, P., Rizzo, A., Dehghanian,

K., Nikolova, M. & Zimmermann, M. 2020 A review of nature-based solutions for urban water management in European circular cities: a critical assessment based on case studies and literature. *Blue-Green Systems* **2** (1), 112–136. doi:10.2166/bgs.2020.932.

Palermo, S. A., Turco, M., Principato, F. & Piro, P. 2019 Hydrological effectiveness of an extensive green roof in Mediterranean climate. *Water* **11** (7), 1378.

Palermo, S. A., Talarico, V. C. & Pirouz, B. 2020 Optimizing rainwater harvesting systems for non-potable water uses and surface runoff mitigation. In: *Numerical Computations: Theory and Algorithms* (Sergeyev, Y. D. & Kvasov, D. E., eds). Springer International Publishing, Cham, pp. 570–582.

Palla, A., Gnecco, I. & Lanza, L. G. 2010 Hydrologic restoration in the urban environment using green roofs. *Water* **2** (2), 140–154.

Pelorosso, R. 2020 Modeling and urban planning: a systematic review of performance-based approaches. *Sustainable Cities and Society* **52**, 101867. https://doi.org/10.1016/j.scs.2019.101867.

Pelorosso, R., Gobattoni, F. & Leone, A. 2018 Increasing hydrological resilience employing nature-based solutions: a modelling approach to support spatial planning. In: *Smart Planning: Sustainability and Mobility in the Age of Change* (Papa, R., Fistola, R. & Gargiulo, C., eds). Springer International Publishing, Cham, pp. 71–82. doi:10.1007/978-3-319-77682-8_5.

Pelorosso, R., La Rosa, D., Floris, S. C. & Cerino, N. 2021a Planning accessible urban green infrastructure for healthy and fair historical towns: the study case of Viterbo, Central Italy. In: *Innovation in Urban and Regional Planning. INPUT 2021. Lecture Notes in Civil Engineering*, Vol. 146 (Rosa, D. L. & Privitera, R., eds). Springer, Cham.

Pelorosso, R., Petroselli, A., Apollonio, C. & Grimaldi, S. 2021b Blue-green roofs: hydrological evaluation of a case study in Viterbo, Central Italy. In: *Innovation in Urban and Regional Planning. INPUT 2021. Lecture Notes in Civil Engineering*, Vol. 146 (Rosa, D. L. & Privitera, R., eds). Springer, Cham.

Recanatesi, F. & Petroselli, A. 2020 Land cover change and flood risk in a peri-urban environment of the metropolitan area of Rome (Italy). *Water Resources Management* **34** (14), 4399–4413. doi:10.1007/s11269-020-02567-8.

Rowe, D. B. 2011 Green roofs as a means of pollution abatement. *Environmental Pollution* **159** (8), 2100–2110. https://doi.org/10.1016/j.envpol.2010.10.029.

Sample, D. J. & Liu, J. 2014 Optimizing rainwater harvesting systems for the dual purposes of water supply and runoff capture. *Journal of Cleaner Production* **75**, 174–194. https://doi.org/10.1016/j.jclepro.2014.03.075.

Santamouris, M. 2014 Cooling the cities–a review of reflective and green roof mitigation technologies to fight heat island and improve comfort in urban environments. *Solar Energy* **103**, 682–703.

Shafique, M., Kim, R. & Lee, D. 2016a The potential of green-blue roof to manage storm water in urban areas. *Nature Environment and Pollution Technology* **15** (2), 715.

Shafique, M., Lee, D. & Kim, R. 2016b A field study to evaluate runoff quantity from blue roof and green blue roof in an urban area. *International Journal of Control and Automation* **9** (8), 59–68.

Solcerova, A., van de Ven, F., Wang, M., Rijsdijk, M. & van de Giesen, N. 2017 Do green roofs cool the air? *Building and Environment* **111**, 249–255. https://doi.org/10.1016/j.buildenv.2016.10.021.

Speak, A. F., Rothwell, J. J., Lindley, S. J. & Smith, C. L. 2012 Urban particulate pollution reduction by four species of green roof vegetation in a UK city. *Atmospheric Environment* **61**, 283–293. https://doi.org/10.1016/j.atmosenv.2012.07.043.

Susca, T., Gaffin, S. R. & Dell'Osso, G. 2011 Positive effects of vegetation: urban heat island and green roofs. *Environmental Pollution* **159** (8–9), 2119–2126.

Takebayashi, H. & Moriyama, M. 2007 Surface heat budget on green roof and high reflection roof for mitigation of urban heat island. *Building and Environment* **42** (8), 2971–2979.

Teston, A., Teixeira, C. A., Ghisi, E. & Cardoso, E. B. 2018 Impact of rainwater harvesting on the drainage system: case study of a condominium of houses in Curitiba, Southern Brazil. *Water* **10** (8), 1100.

Treppiedi, D., Cipolla, G., Francipane, A. & Noto, L. 2021 Detecting precipitation trend using a multiscale approach based on quantile regression over a Mediterranean area. *International Journal of Climatology* **41**, 5938–5955.

UN 2018 *United Nations Final Report on World Urbanization Prospects 2018*.

van den Bosch, M. & Ode Sang, Å. 2017 Urban natural environments as nature-based solutions for improved public health – a systematic review of reviews. *Environmental Research* **158**, 373–384. https://doi.org/10.1016/j.envres.2017.05.040.

van der Meulen, S. H. 2019 Costs and benefits of green roof types for cities and building owners. *Journal of Sustainable Development of Energy, Water and Environment Systems* **7** (1), 57–71.

Viola, F., Hellies, M. & Deidda, R. 2017 Retention performance of green roofs in representative climates worldwide. *Journal of Hydrology* **553**, 763–772. doi:10.1016/j.jhydrol.2017.08.033.

Xie, J., Luo, S., Furuya, K. & Sun, D. 2020 Urban parks as green buffers during the COVID-19 pandemic. *Sustainability* **12** (17), 6751.

Yang, J., Yu, Q. & Gong, P. 2008 Quantifying air pollution removal by green roofs in Chicago. *Atmospheric Environment* **42** (31), 7266–7273. https://doi.org/10.1016/j.atmosenv.2008.07.003.

Zhang, X. & Hu, M. 2014 Effectiveness of rainwater harvesting in runoff volume reduction in a planned industrial park, China. *Water Resources Management* **28** (3), 671–682. doi:10.1007/s11269-013-0507-9.

First received 22 September 2021; accepted in revised form 25 July 2022. Available online 8 August 2022